Fabrication and characterization of a microporous polymeric micro-filter for isolation of *Cryptosporidium parvum* oocysts

J. Micromech. Microeng. **21** (2011) 035002 (8pp) doi:10.1088/0960-1317/21/3/035002

Fabrication and characterization of a microporous polymeric micro-filter for isolation of *Cryptosporidium parvum* oocysts

Majid Ebrahimi Warkiani, Chao-Ping Lou and Hai-Qing Gong[1]

School of Mechanical and Aerospace Engineering, Nanyang Technological University, 50 Nanyang Avenue, Singapore 639798

E-mail: mhqgong@ntu.edu.sg

Received 12 October 2010, in final form 16 December 2010
Published 1 February 2011
Online at stacks.iop.org/JMM/21/035002

Abstract
A rapid and effective method to concentrate *Cryptosporidium parvum* oocysts present in large volumes of drinking water into smaller volumes is critical for accurate detection and quantification of *C. parvum* oocysts from drinking water. Filtration-based concentration techniques have been widely used to recover *C. parvum* oocysts into a small volume for downstream analysis. We present a rapid method for fabrication of a polymeric micro-filter with ordered pores and a smooth surface using UV lithography and MEMS technology. To support the filter membrane, we also developed a technique for integrated fabrication of a support mesh. We demonstrated that the filter is able to isolate the oocysts which can be further detected using fluorescent techniques. Sample loading and back-flushing using the micro-filter resulted in 95–99% recovery with a concentration ratio above 2000 of the spiked *C. parvum* oocysts, which showed significantly improved performance compared with current commercial filters.

(Some figures in this article are in colour only in the electronic version)

1. Introduction

Cryptosporidium parvum oocyst is a parasite commonly found in surface waters such as lakes and rivers, especially when the water is in contact with animal wastes and sewage. The highly infectious nature of *C. parvum* oocyst and the lack of effective medication until now urge a reliable routine test to monitor *C. parvum oocyst* contamination in the drinking water supply system [1]. Available bio-sensors only detect microorganisms which are directly in contact with the sensor region; hence, detection of low concentration bacteria in a large volume is hard because there is low possibility for bacteria to interact with the sensitive zone of the biosensor [2]. Consequently, a reliable method to concentrate *C. parvum* oocysts present in large volumes of drinking water into smaller volumes is crucial for accurate detection and quantification of *C. parvum* oocysts from drinking water. Filtration techniques have been widely used to recover *C. parvum* oocysts into a small volume for downstream analysis [3]. Commercial micro-filters cannot be used effectively for this purpose because they suffer from several drawbacks like tortuous pore path, low pore density and high coefficient of variation (CV > 20%) [4].These micro-structural defects normally lead to a poor cell recovery rate [5] and also low throughput.

Micro-fabricated membranes that contain pores with the same size and shape can overcome these micro-structural defects. The fabrication process allows enough flexibility to control the porosity and the pore size and shape according to desired application (e.g. bacteria separation and recovery) in order to have higher flow rate, lower clogging ratio, better recovery and enough reliability. In recent years, different methods have been proposed to create membranes with cylindrical pores like laser interference lithography and silicon

[1] Author to whom any correspondence should be addressed.

micro machining technology [6], aperture array lithography [7], nanoimprinting using an alumina template [8], excimer lasers [9], phase separation micromolding [10], and more recently a dissolving mold technique [11]. In some studies, micro-fabricated filters were used successfully for separation [12, 13] and fractionation [14] purposes.

In this study, we present a method for rapid fabrication of a polymeric micro-filter using conventional lithography and MEMS techniques. We also explain how to release the membrane from the substrate successfully. This filter is used for capturing and recovering of *C. parvum* oocysts from the prepared water samples. Since the size of *C. parvum* oocyst is between 3 and 6 μm, we chose 1.5 and 2.5 μm pore size for the micro-fabricated filter in order to achieve a higher filtration flux and better recovery in comparison to the cellulose membrane filter (1.2 μm) or Envirochek HV (1 μm). The obtained results indicate successful isolation of *C. parvum* oocyst on the membrane surface. When a 15 s backwash was applied, the micro-fabricated membrane filter showed superior performance to other filters for recovery of oocysts with a 95–99% recovery rate.

2. Materials and methods

2.1. Fabrication of perforated polymeric membrane

The schematic representation of the entire fabrication process is illustrated in figure 1. First, a silicon substrate, ⟨1 0 0⟩, p-type, 100 mm in diameter, was cleaned in a piranha solution (96% H_2SO_4 and 30% H_2O_2) for 25 min at 120 °C to remove any organic contaminations on the wafer surface. Then, the substrate was submerged in the buffered oxide etchant (BOE) for 2 min to clean the natural oxide layer. After rinsing with DI water and drying with N_2 gas, the dehydration bake step was performed in a Suss machine (Delta 150 VPO) for 2 min. To facilitate the release of the membrane from the substrate, a thin sacrificial layer of polystyrene film (Sigma-Aldrich) of 2 μm thickness was spin coated on the silicon wafer and cured on a hotplate at 90 °C for 10 min. After curing the sacrificial layer (i.e. polystyrene film) and cooling down the wafer to the room temperature, a 4 μm thin layer of SU-8 photoresist (SU-8 2005, MicroChem Corp.) was spin coated on the top of cured sacrificial film.

After soft baking the SU-8 on the hotplate, a chrome-coated quartz mask with circular, square and rectangular features (1.5 and 2.5 μm openings) was used to transfer the patterns to the SU-8 photoresist layer. UV-lithography was then carried out using a Karl Suss MA6 mask aligner (Karl Suss) in a vacuum contact mode between the silicon wafer and the mask at 365 nm wavelength. Then SU-8 was kept again on the hotplate for 5 min for post-exposure purpose at 95 °C and cooled down to room temperature gradually. In this step, the cationic photo-polymerization of the epoxy occurred in SU-8 resist. Finally, the exposed resist layer was developed by immersion of the whole wafer inside the SU-8 developer (MicroChem Corp.) with manual agitation for 2 min. After development, the sample was rinsed with isopropyl alcohol (IPA) and subsequently dried with N_2 gas. The resulting structure is an array of circular and rectangular holes with different sizes registered across the SU-8 film. Figure 2(*a*) shows the SEM image of a thorough-hole membrane, in which an array of rectangular pores were successfully formed in the SU-8 film.

2.2. Fabrication of support structure

The perforated SU-8 film is too thin to be used directly for water filtration applications, and it also folds easily upon release from the wafer substrate; therefore, we constructed a backside support with larger openings using a thick layer of SU-8. For this purpose, a second layer of SU-8 (SU-8 2015, MicroChem Corp.) film with thickness of 20 μm was spin coated on top of the first layer. After soft baking on the hotplate for around 45 min, second exposure through a plastic mask was carried out to form the support layer with 600 μm apertures in the backside of the membrane. After second exposure, the substrate was held on the hotplate for 40 min for post-exposure and also good adhesion of the second layer to the first layer. Subsequently, it was cooled down to the room temperature and was developed in a SU-8 developer for 5 min with manual agitation. The resulting structure is represented in figure 2(*b*).

2.3. Release of polymeric membrane

The most important impediment in fabrication of the polymeric micro-filter with this method is the release of the membrane from the substrate without membrane failure. The backside support [6, 7] helps the membrane stay flat upon release from the substrate, but the large thickness of support structure may cause the entire structure to collapse and adhere to the substrate while the sacrificial layer dissolves in the appropriate solvent. Therefore, finding a suitable material to be used as a sacrificial layer for the releasing step is an important issue. In the literature, some methods have been proposed for this purpose, including sputtering (or electroplating) copper [15] or chromium [16] as a sacrificial layer beneath the SU-8 film and etching the metal film in the final step. Using metals like copper or chromium may require extra steps such as sputtering, and also use of toxic material as an etchant for sacrificial layer removal. In contrast, we can employ appropriate polymers and solvents for releasing purpose. Table 1 shows a list of materials that were used as a sacrificial layer in this study. All the solvents have no effect on the cured SU-8 film. We found that AZ 9260 and polystyrene [17] presented better results in the releasing step regarding the film quality and complete dissolution in the solvent.

Depending on the thickness of the backside support layer and the sacrificial layer in use, it typically takes between 10 and 20 min to release the membrane from the substrate in the pertinent solvent. Ultrasonic agitation (low frequency ≈ 20 kHz) is required for releasing the membrane from the substrate because, firstly, it expedites the releasing process and secondly, it prevents the adhesion of SU-8 film to the substrate when the sacrificial layer dissolves in the solvent. It is noted that the openings of the support mesh must be large enough to avoid causing any significant effect on the total hydraulic resistance to flow across the membranes [7].

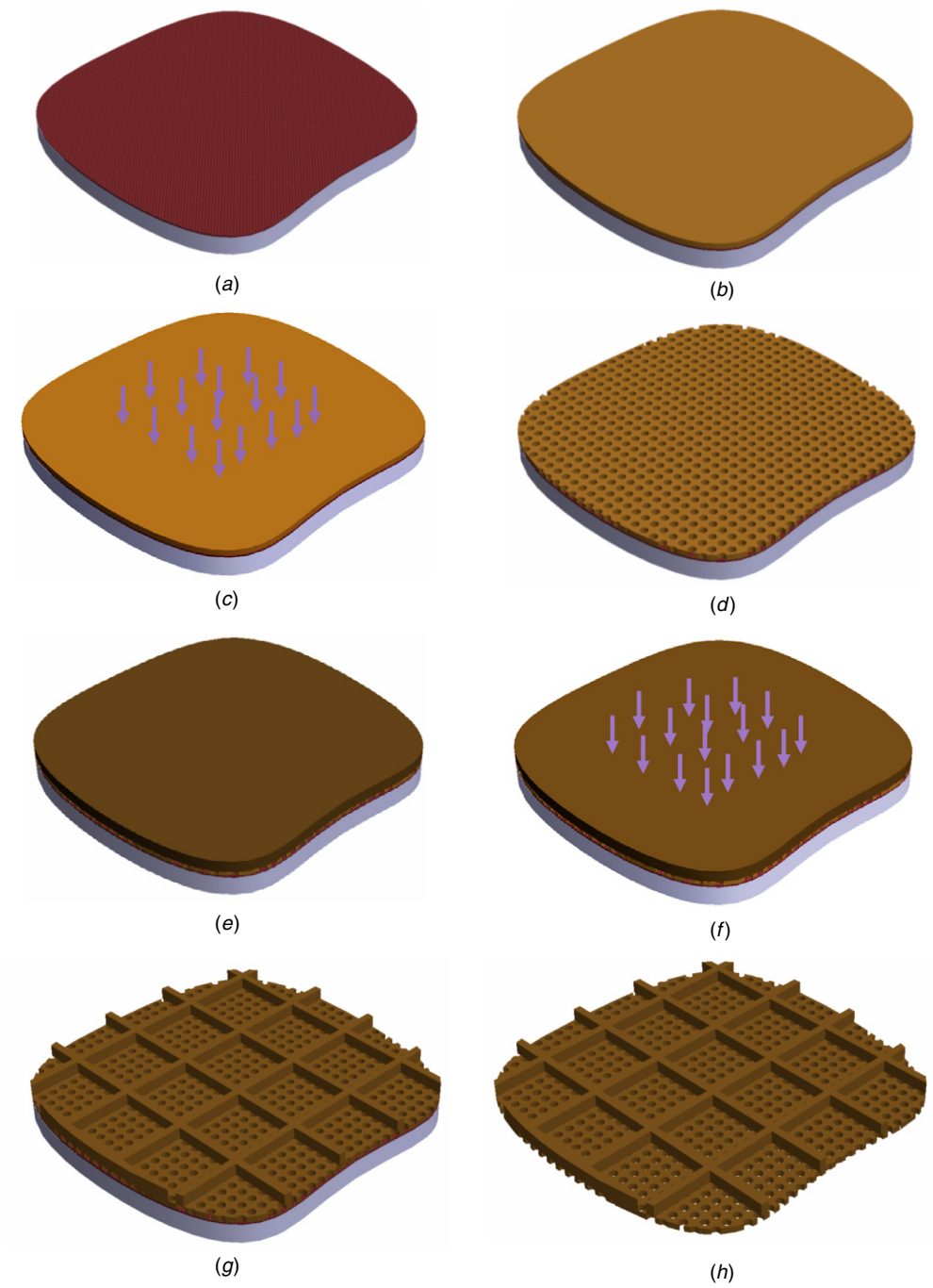

Figure 1. Schematic representation of the fabrication process for the polymeric micro-filter with an integrated support mesh, (*a*) spin-coating of a thin sacrificial layer, (*b*) spin-coating of a thin SU-8 layer, (*c*) first UV-exposure through a quartz mask, (*d*) development to obtain a perforated thin filter layer, (*e*) spin-coating of a thick SU-8 layer, (*f*) second UV-exposure through a plastic mask, (*g*) formation of a support layer made of a thick SU-8 film after second development, and (*h*) the final micro-filter with a support mesh after releasing from the wafer substrate.

Table 1. Materials and process conditions used for release of the micro-filter from the substrate.

Material	Solvent	Curing process	Release step
AZ 9260	Acetone	Thickness 2 μm @ 110 °C for 20 min	Immersion in acetone bath for 15 min (with ultrasonic agitation)
PMMA	Chloroform	Thickness 2 μm @ 95 °C for 25 min	Immersion in chloroform bath for 5 min (with ultrasonic agitation)
Polystyrene	Toluene	Thickness 2 μm @ 90 °C for 10 min	Immersion in toluene bath for 15 min (with manual agitation)
Polyurethanes	DMF	Thickness 2 μm @ 80 °C for 30 min	Immersion in DMF bath for 15 min (with ultrasonic agitation)

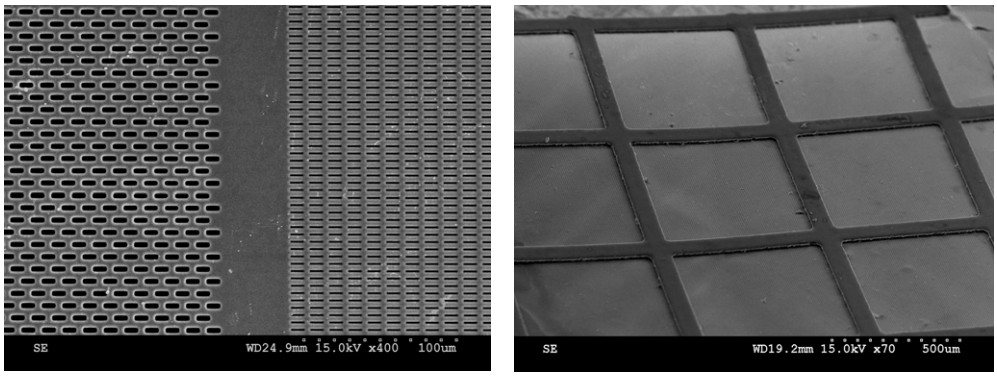

(*a*) (*b*)

Figure 2. (*a*) SEM image of a micro-filter with an array of rectangular pores, (*b*) SEM image of the membrane with an integrated support mesh.

3. Results

3.1. Membrane properties

By employing a conventional lithography technique, we demonstrated a simple and rapid process for fabrication of micro-filters for biological applications including waterborne pathogen removal and concentration from drinking water. In this study, we employed SU-8 resist for making the filter due to its wide use as a structural layer and its biocompatibility [18], and its good thermal and chemical stability.

The measurement of the pore-size distribution of the SU-8 filter membranes was carried out using digitalized photographs from the HITACHI S3500 scanning electron microscope, which is equipped with the 'in-built dimension measurement' module and image analysis program SEMICAPS 2200 (Semicaps Pte Ltd) from random regions of the samples. The mean pore diameters are 1.5 and 2.5 μm (for different patterns) and standard deviations are 100 and 90 nm, respectively. Therefore, the corresponding coefficient of variation (CV $= \sigma/\mathrm{M}$) is 6.6% and 3.6%, respectively. In the dense region of filter membranes, a pore density of about 7×10^7 pores cm^{-2} is achieved. The CV and pore density of our membrane are much higher than in the commercial ones like the polymeric track-etched membrane with CV and an average pore density of around 20% and 10^7 pores cm^{-2}, respectively [4].

The mechanical strength of the membrane depends on the thickness of the membrane, Young's modulus of membrane, the intrinsic tensile stress, the shape and distribution of the pores and the distance between the bars of support structure [6]. Van Rijn *et al* [19] proposed the following correlation for calculation of the maximum load of the perforated membrane:

$$P_{\max} = 0.58 \frac{h\sigma_{\mathrm{yeff}}^{1.5}}{l E_{\mathrm{eff}}^{0.5}}$$

where $P_{\max}$ is the maximum load, h is the membrane thickness, l is the distance between the support bars, E_{eff} and σ_{yeff} are the effective Young's modulus and yield strength, respectively. The porosity in this model is considered by a factor $(1-K)$ for calculation of E_{eff} and σ_{yeff}, where K is the porosity. By choosing $h = 4$ μm, $l = 600$ μm, $E = 2$ GPa [20], $\sigma_{\mathrm{yeff}} = 60$ MPa [20], $K = 25\%$ and $E_{\mathrm{eff}} = (1\text{–}0.25) \times E$ for the parameters of the micro-fabricated membrane, the burst pressure would be 53 kPa (0.53 bar), which is enough for most microfiltration processes.

Finite element simulation was also used in this work to investigate the stress distribution and maximum load in the polymeric micro-filter with different frame sizes (backside support). Figure 3 depicts that the largest stress is located at the middle of the edge because the total tensile stress at the edge is the addition of the constant tensile stress due to stretching and the bending stress near the middle of the edge [19]. At the center, the membrane also experiences the highest bending stress. Those holes which are located near the ring also experience maximum stress, especially around the corners of each hole. For a specified pressure, the deflection of perforated membranes is around 7% larger than for non-perforated membranes. The perforation distribution has no significant influence on the mechanical stability of the membrane, but the aperture size of backside support has a significant influence on the membrane strength.

In addition, a membrane with higher porosity deflects more than a membrane with lower porosity. The FEM results also confirm that the maximum stress is approximately proportional to the applied pressure.

In addition to the square-shape support mesh, we also employed hexagonal openings to better profit from the membrane surface. Their dimensions depend on the thickness of the micro-fabricated membrane and on the pressure of the filtration process. For higher pressures and thinner membranes, the dimensions of the hexagons should be smaller [19].

Figure 4 shows the SEM photo of a membrane which was broken during the filtration. This photo also confirms that the rupture occurs in the center and middle of the membrane edges, where the stress is maximal.

3.2. Integrity test with mono-sized microbeads

In general, direct integrity testing is defined as a 'physical test' that is able to detect and isolate integrity breach [21]. Direct integrity testing represents the most accurate means of assessing the integrity of a membrane filtration system which can be done by a marker-based test. Marker-based tests employ

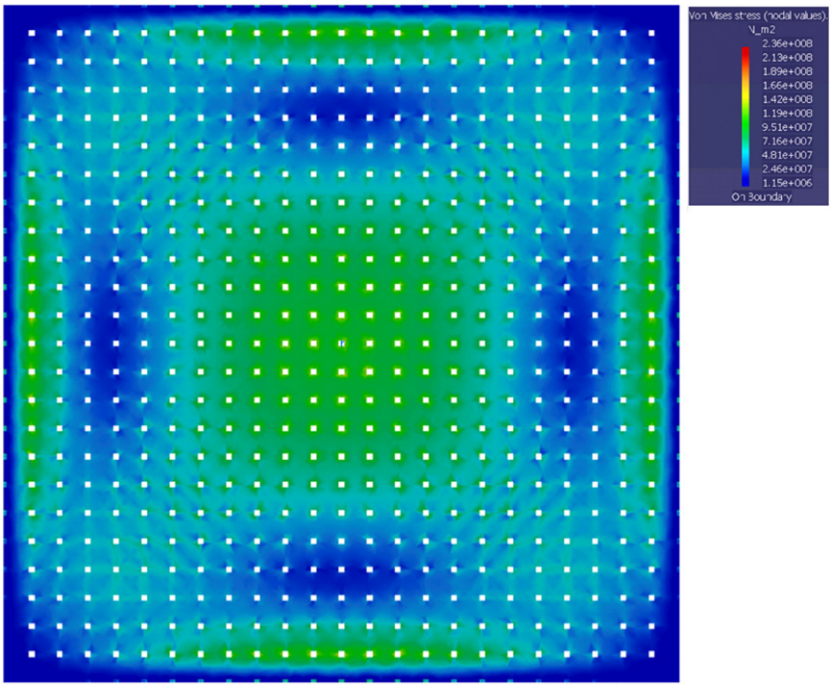

Figure 3. FEM simulation of the stress distributions of perforated membranes, in which only the membrane within one support mesh element (600 × 600 μm) is shown.

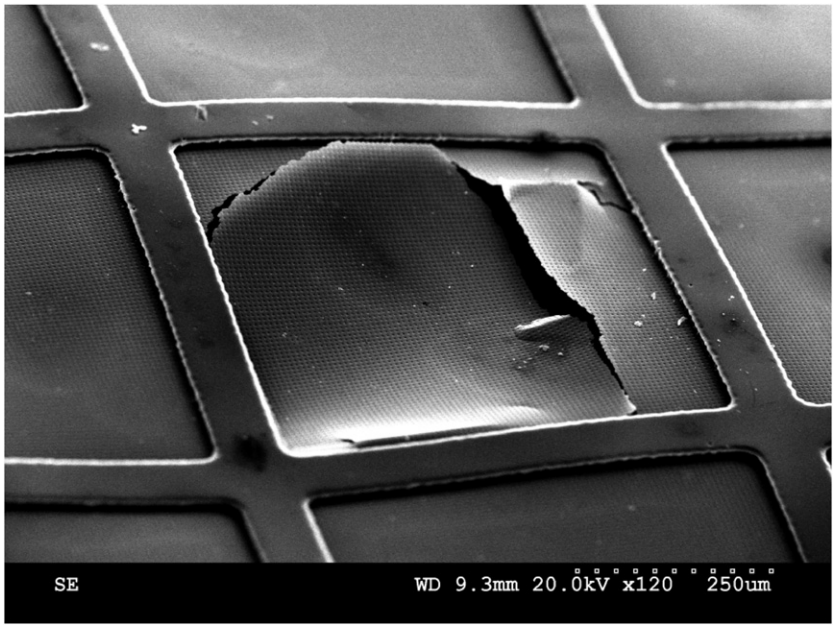

Figure 4. SEM photograph of a broken membrane which shows the rupture occurs at the points of maximum stress.

either a spiked particulate or a molecular marker to verify membrane integrity by directly assessing the removal of the marker. The recommended surrogate for *C. parvum* oocysts must have an effective size of 3 μm or smaller [21]. For this purpose, filtration of suspensions of microbeads of precise diameters has been carried out. First, a test solution with spherical polystyrene particles of 3 μm size was prepared and filtered through the membrane by a dead-end filtration (DEF) setup under a constant pressure. Then, the permeate solution filtered for the second time through an Anopore aluminum membrane (cat no: 6809-5022, Whatman) with nominal pore size of 0.2 μm to capture any microbeads that may have passed from the polymeric micro-filter. Subsequently, the surface of the aluminum membrane was fully observed under the microscope, and it was realized that no beads passed through the polymeric micro-filter. Figure 5(*a*) shows the SEM photo of the polymeric filter which fully captured the spherical beads. In order to check the recovery rate, the polymeric micro-fabricated filter was backflushed with pure water to remove the beads from the surface. The results of the optical

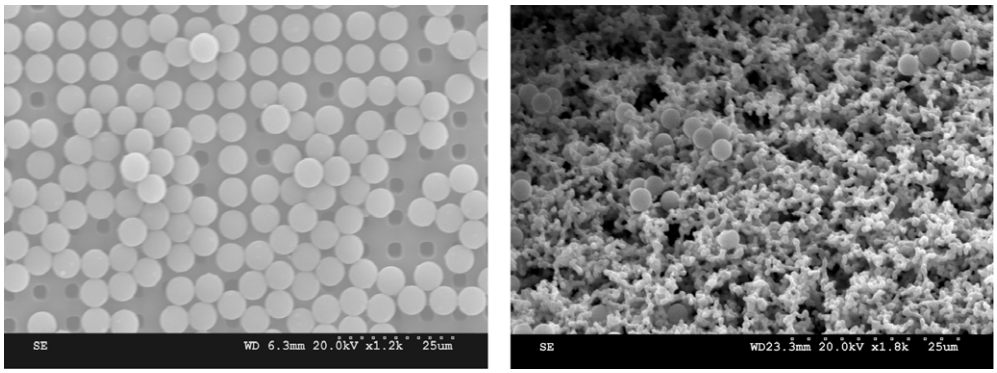

(*a*) (*b*)

Figure 5. (*a*) SEM photo of a polymeric micro-fabricated filter with captured microbeads on its surface, (*b*) SEM photo of trapped beads inside the tortuous structures of the cellulose membrane.

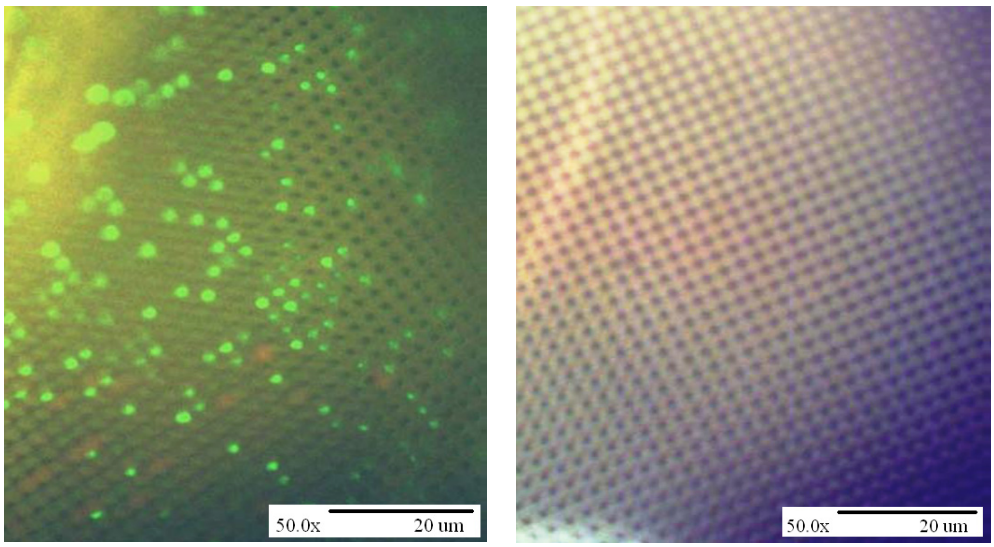

(*a*) (*b*)

Figure 6. Microscopic images of a polymeric micro-fabricated membrane, (*a*) after filtration, where the green particles are the fluorescently labeled oocysts captured, (*b*) after backflush.

observation showed that more than 99% of microbeads were recovered.

A similar integrity test was performed for the cellulose acetate membrane (cat no: 1040-3012, Whatman), which is widely used in industry for cell capturing purpose. The result shows that more than 50% of microbeads were trapped between the tortuous structures of the membrane and could not be recovered after the backflush step. Figure 5(*b*) depicts the SEM photo of the trapped beads inside the cellulose membrane.

3.3. Recovery test with C. parvum oocyst

The recovery rate of the polymeric micro-fabricated filter was also evaluated by comparing with the Millipore cellulose acetate membrane (pore size of 1.2 μm) which is normally used for clarification of aqueous solutions and microorganism (e.g. *C. parvum oocyst*) removal. For this purpose, heat-inactivated *C. parvum* oocysts (Waterborne Inc., New Orleans, LA, USA), which were labeled with Crypt-a-Glo antibody, were spiked into 10 ml pure water and two identical samples were prepared. Then, each membrane was mounted onto the holder and the samples were passed through the filters, while permeates collected in two waste-liquid bottles separately. Then, permeates from the micro-fabricated filter went through to a subsequent filtration step with the Anopore aluminum membrane filter to capture any oocyst that might pass through the micro-fabricated filter. The *C. parvum* oocysts captured by the micro-fabricated filter were observed under a fluorescence microscope by the FITC (fluorescence isothiocyanate) technique (Waterborne. Inc., New Orleans, LA, cat no. A400FLK). Figure 6(*a*) shows the surface of the micro-fabricated filter after filtration. It can be seen that nearly all oocysts are captured by the filter. A clean surface of the aluminum membrane filter as observed under the microscope indicates that no oocysts passed through the micro-fabricated filter. *C. parvum* oocysts were recovered from the micro-filters by backflush using a 10 ml backflush buffer solution containing 1% sodium polyphosphate (NaPP) and 0.1% Tween 80. Figure 6(*b*) depicts the surface of the polymeric micro-filter

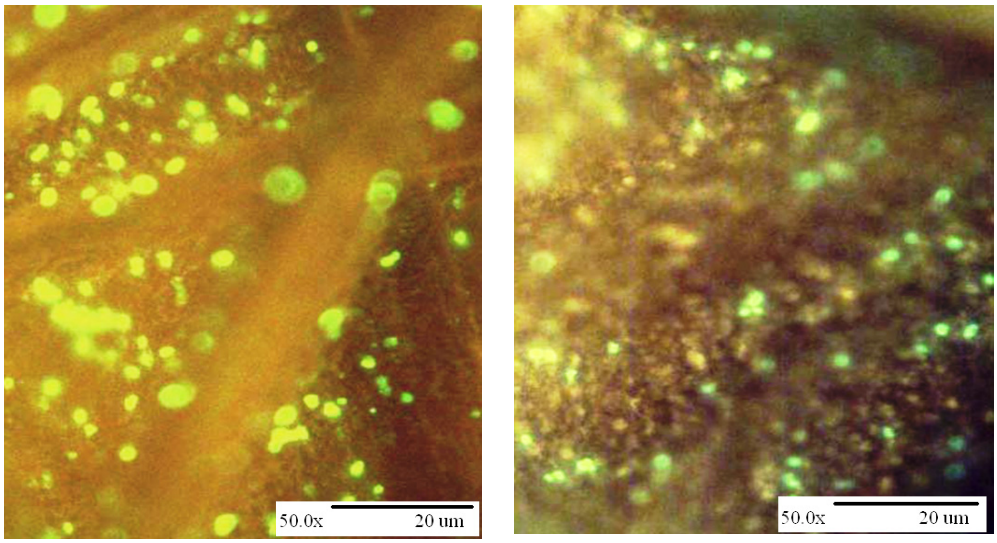

(*a*) (*b*)

Figure 7. Microscopic images of a cellulose acetate membrane, (*a*) after filtration, (*b*) after backflush. The green particles are the fluorescently labeled oocysts captured.

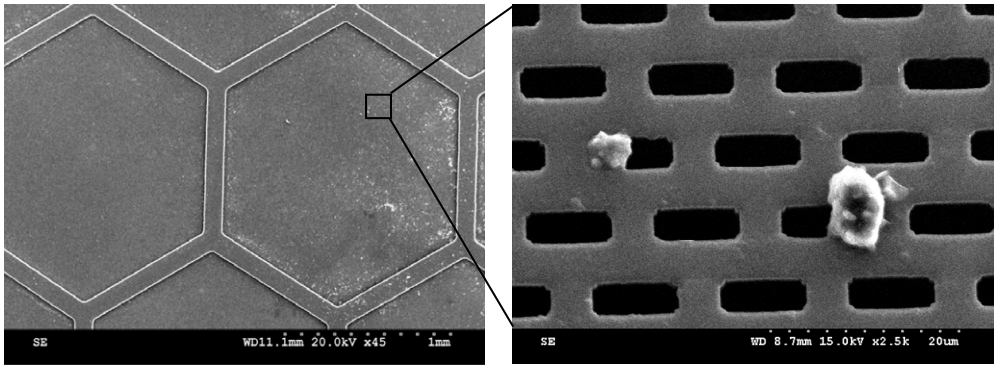

(*a*) (*b*)

Figure 8. (*a*) A SEM image of a polymeric micro-fabricated membrane with a honey-comb support mesh after filtration, (*b*) a close-up view of the membrane surface which shows the captured *C. parvum* oocysts.

after the backflush step. Nearly all oocysts were recovered from the polymeric micro-fabricated filter. For the cellulose membrane, it was observed that (see figure 7) a large amount of *C. parvum* oocysts still adhered to the filter after backflush with the same backflush buffer.

The same experiments have been performed to compare and evaluate the recovery performance of the polymeric micro-fabricated filter and the Envirochek HV filter (cat no: 12099, Pall Corp.). The obtained results indicate that the micro-fabricated membrane filter with a 95–99% recovery rate was superior to Envirochek HV which showed a recovery rate of 60%. Unique features of the polymeric micro-fabricated filter like the smooth surface, straight pore path and uniform pore-size greatly reduce the oocyst adhesion to the filter surface and enable us to achieve a very high recovery rate (up to 99%) of *C. parvum* oocysts when applying backflush. In addition, the images of the micro-fabricated filter after backflush shows that the filter surface is clean and had been restored to its original condition, which indicates high reusability of the filter.

A SEM photo of the polymeric membrane with a honey-comb support mesh after filtration is also depicted in figure 8(*a*). The close-up view in figure 8(*b*) shows the trapped *C. parvum* oocysts between the pores, which confirms that the mono-pore and the smooth surface of the membrane result in better results in comparison to the commercial membranes (i.e. cellulose acetate membrane) for the oocyst concentration applications.

4. Conclusion

In the present work, we explained a method for fabrication of a polymeric micro-filter membrane with an integrated support mesh. This method can be used to fabricate micro-filters with different pore sizes and shapes, smooth membrane surfaces and high porosities to isolate microorganisms such as *C. parvum* oocysts. Isolated microorganisms can be detected subsequently using various available techniques. The results demonstrate that all the captured oocysts can be easily recovered from the surface of the filter by a backflush, and the membrane can be reused. In addition, the oocysts can be directly detected on the surface of the membrane using a standard immunoassay. Micro-fabricated filters are also

appropriate for many other applications like filtration of white blood cells (leukocytes) from blood-cell concentration, cell analysis, yeast harvesting and healthcare.

Acknowledgment

The authors acknowledge the financial support of the Environment & Water Industry Programme Office of Singapore under the project grant MEWR C651/06/149.

References

[1] Inoue M, Rai S K, Oda T, Kimura K, Nakanishi M, Hotta H and Uga S 2003 A new filter-eluting solution that facilitates improved recovery of *Cryptosporidium oocysts* from water *J. Microbiol. Methods* **55** 679–86

[2] Noble R T and Weisberg S B 2005 A review of technologies for rapid detection of bacteria in recreational waters *J. Water Health* **3** 381–92

[3] Dubitsky A, DeCollibus D and Ortolano G A 2002 Sensitive fluorescent detection of protein on nylon membranes *J. Biochem. Biophys. Methods* **51** 47–56

[4] Ramachandran V and Fogler H S 1999 Plugging by hydrodynamic bridging during flow of stable colloidal particles within cylindrical pores *J. Fluid Mech.* **385** 129–56

[5] Wohlsen T, Bates J, Gray B and Katouli M 2004 Evaluation of five membrane filtration methods for recovery of Cryptosporidium and Giardia isolates from water samples *Appl. Environ. Microbiol.* **70** 2318–22

[6] Kuiper S, Van Rijn C J M, Nijdam W and Elwenspoek M C 1998 Development and applications of very high flux microfiltration membranes *J. Membr. Sci.* **150** 1–8

[7] Han K, Xu W, Ruiz A, Ruchhoeft P and Chellam S 2005 Fabrication and characterization of polymeric microfiltration membranes using aperture array lithography *J. Membr. Sci.* **249** 193–206

[8] Yanagishita T, Nishio K and Masuda H 2007 Polymer through-hole membrane fabricated by nanoimprinting using metal molds with high aspect ratios *J. Vac. Sci. Technol.* B **25** L35–8

[9] Saxena I, Agrawal A and Joshi S S 2009 Fabrication of microfilters using excimer laser micromachining and testing of pressure drop *J. Micromech. Microeng.* **19** 025025

[10] Gironès M, Akbarsyah I J, Nijdam W, van Rijn C J M, Jansen H V, Lammertink R G H and Wessling M 2006 Polymeric microsieves produced by phase separation micromolding *J. Membr. Sci.* **283** 411–24

[11] Chen L, Ebrahimi Warkiani M, Liu H B and Gong H Q 2010 Polymeric micro-filter manufactured by a dissolving mold technique *J. Micromech. Microeng.* **20** 075005

[12] Kuiper S, Van Rijn C, Nijdam W, Raspe O, Van Wolferen H, Krijnen G and Elwenspoek M 2002 Filtration of lager beer with microsieves: flux, permeate haze and in-line microscope observations *J. Membr. Sci.* **196** 159–70

[13] Yang X, Yang J M, Tai Y C and Ho C M 1999 Micromachined membrane particle filters *Sensors Actuators* A **73** 184–91

[14] Brans G, Schroën C G P H, van der Sman R G M and Boom R M 2004 Membrane fractionation of milk: state of the art and challenges *J. Membr. Sci.* **243** 263–72

[15] Yi F, Tang E, Zhang J and Xian D 2000 A new sacrificial layer method of LIGA technology to fabricate movable part of a gripper *Microsyst. Technol.* **6** 154–6

[16] Calleja M, Tamayo J, Johansson A, Rasmussen P, Lechuga L and Boisen A 2003 Polymeric cantilever arrays for biosensing applications *Sensor Lett.* **1** 1–5

[17] Luo C, Govindaraju A, Garra J, Schneider T, White R, Currie J and Paranjape M 2004 Releasing SU-8 structures using polystyrene as a sacrificial material *Sensors Actuators* A **114** 123–8

[18] Voskerician G, Shive M S, Shawgo R S, Von Recum H, Anderson J M, Cima M J and Langer R 2003 Biocompatibility and biofouling of MEMS drug delivery devices *Biomaterials* **24** 1959–67

[19] Van Rijn C, Van Der Wekken M, Nijdam W and Elwenspoek M 1997 Deflection and maximum load of microfiltration membrane sieves made with silicon micromachining *J. Microelectromech. Syst.* **6** 48–54

[20] Becker H and Gärtner C 2008 Polymer microfabrication technologies for microfluidic systems *Anal. Bioanal. Chem.* **390** 89–111

[21] Leonard B 2003 *Membrane Filtration Guidance Manual* US Environmental Protection Agency, Office of Water